The SunCHECK™ Platform powers Quality Management in radiation therapy.

Scalable to meet the needs of any clinic or network, SunCHECK helps:

- **Reduce risks**
- **Control costs**
- **Improve treatment quality**

Visit sunnuclear.com to learn how SunCHECK fits into your clinic.

Patient Safety Starts Here

SUN NUCLEAR corporation

Important pharmacokinetic parameters for individualization of ^{177}Lu-PSMA therapy: A global sensitivity analysis for a physiologically-based pharmacokinetic model

Deni Hardiansyah
Medical Physics and Biophysics, Physics Department, Faculty of Mathematics and Natural Sciences, Universitas Indonesia, Depok 16424, Indonesia

Peter Kletting
Medical Radiation Physics, Department of Nuclear Medicine, Ulm University, Ulm 89081, Germany
Department of Nuclear Medicine, Ulm University, Ulm 89081, Germany

Nusrat J. Begum
Medical Radiation Physics, Department of Nuclear Medicine, Ulm University, Ulm 89081, Germany

Matthias Eiber
Department of Nuclear Medicine, Klinikum rechts der Isar, Technische Universität München, München 81675, Germany

Ambros J. Beer
Department of Nuclear Medicine, Ulm University, Ulm 89081, Germany

Supriyanto A. Pawiro
Medical Physics and Biophysics, Physics Department, Faculty of Mathematics and Natural Sciences, Universitas Indonesia, Depok 16424, Indonesia

Gerhard Glatting[a)]
Medical Radiation Physics, Department of Nuclear Medicine, Ulm University, Ulm 89081, Germany
Department of Nuclear Medicine, Ulm University, Ulm 89081, Germany

(Received 29 July 2020; revised 26 October 2020; accepted for publication 13 November 2020; published 15 December 2020)

Purpose: The knowledge of the contribution of anatomical and physiological parameters to interindividual pharmacokinetic differences could potentially be used to improve individualized treatment planning for radionuclide therapy. The aim of this study was therefore to identify the physiologically based pharmacokinetic (PBPK) model parameters that determine the interindividual variability of absorbed doses (ADs) to kidneys and tumor lesions in therapy with ^{177}Lu-labeled PSMA-targeting radioligands.
Methods: A global sensitivity analysis (GSA) with the extended Fourier Amplitude Sensitivity Test (eFAST) algorithm was performed. The whole-body PBPK model for PSMA-targeting radioligand therapy from our previous studies was used in this study. The model parameters of interest (input of the GSA) were the organ receptor densities $[R_0]$, the organ blood flows f, and the organ release rates λ. These parameters were systematically sampled NE times according to their distribution in the patient population. The corresponding pharmacokinetics were simulated and the ADs (model output) to kidneys and tumor lesions were collected. The main effect S_i and total effect S_{Ti} were calculated using the eFAST algorithm based on the variability of the model output: The main effect S_i of input parameter i represents the reduction in variance of the output if the "true" value of parameter i would be known. The total effect S_{Ti} of an input parameter i represents the proportion of variance remaining if the "true" values of all other input parameters except for i are known. The numbers of samples NE were increased up to 8193 to check the stability (i.e., convergence) of the calculated main effects S_i and total effects S_{Ti}.
Results: From the simulations, the relative interindividual variability of ADs in the kidneys (coefficient of variation CV = 31%) was lower than that of ADs in the tumors (CV up to 59%). Based on the GSA, the most important parameters that determine the ADs to the kidneys were kidneys flow ($S_i = 0.36$, $S_{Ti} = 0.43$) and kidneys receptor density ($S_i = 0.25$, $S_{Ti} = 0.30$). Tumor receptor density was identified as the most important parameter determining the ADs to tumors (S_i and S_{Ti} up to 0.72).
Conclusions: The results suggest that an accurate measurement of receptor density and flow before therapy could be a promising approach for developing an individualized treatment with ^{177}Lu-labeled PSMA-targeting radioligands. © *2020 The Authors. Medical Physics* published by Wiley Periodicals LLC on behalf of American Association of Physicists in Medicine [https://doi.org/10.1002/mp.14622]

Key words: absorbed dose, eFAST, GSA, PBPK model, PSMA

1. INTRODUCTION

Radionuclide treatment is expected to be improved by an individualized treatment planning approach, that is by considering the individual pharmacokinetics.[1–4] In radioligand therapy it has been shown that the interindividual variability of the internal absorbed doses (ADs) might be introduced by from several sources, for example, biokinetic parameters.[4–6] Some of these parameters might be measured/estimated prior to therapy and allow adjustment of the injected activity and ligand amount.[3,7–9] However, quantitative analyses of the contribution of these parameters to the interindividual variability of ADs are not available. Such quantitative analyses can be conducted using sensitivity analysis (SA).

For model development, knowledge of the variability of the model output in relation to the model input is essential. By definition, sensitivity analysis examines how the variability of a model's output can be attributed to the variabilities of the model's input.[10,11] Based on the results of the SA, strategies can then be developed to reduce the variability of output. SA allows to identify the most important input parameter, for example, individual anatomical and physiological parameters (as used in mathematical physiologically based pharmacokinetic (PBPK) models), which have a large effect to the model output, for example, to the ADs. In general, SA methods can be grouped into two categories: (a) local methods that consider sensitivities related to a specific set of input parameter values, and (b) global methods, which calculate the contribution of a parameter over the set of all possible input parameters.

Recently, a variance-based global sensitivity analysis (GSA) using the Sobol method has been used to investigate the effect of interindividual variabilities of the time-integrated activity coefficients (TIACs) and S-values to the calculation of the organ ADs of ^{18}F-FSPG using the MIRD formalism.[4] The interindividual variability of the TIACs and S-values was computed from the individual TIAC data of five volunteers (the coefficients of variation CV of the organs ranged from 10% to 57%) and from the individual phantom-specific sets of S-values of six human computational phantoms (the CVs of various pairs of the organs ranged from 0.24% to 206%).[4] As a result, an accurate determination of individual TIACs was shown to possibly decrease the interindividual variability of the ADs in the population (around 90% for the interindividual variability of ADs in the kidneys based on the main effect S_i value) while the S-values contributed less to the AD interindividual variability (less than 10% for the interindividual variability of ADs in the kidneys based on the main effect S_i value).[4] However, the source of the interindividual variability of the TIACs (which strongly affects the calculation of ADs interindividual variability) was not investigated. The knowledge of the main anatomical and physiological parameters defining/determining the interindividual differences would possibly allow an individual treatment planning considering the trade-off between patient load/costs and gain in treatment efficacy (i.e., ADs) based on the needed measurements. Thus, a systematic study on this topic is needed.

Individual TIACs are usually determined by fitting the biokinetic data with a sum of exponential functions[12,13] or a physiologically based pharmacokinetic (PBPK) model.[8,14] Previously, we showed that the implementation of a PBPK model for dosimetry has advantages over the sum of exponential functions in the number of data per fitted parameter.[15] Furthermore, PBPK models have been shown to be a powerful tool to simulate the biokinetics of radiolabeled drugs and to predict both organ TIACs and ADs during peptide-receptor radionuclide therapy, radioimmunotherapy and radioligand therapy.[3,9,16,17] Unlike the sum of exponential functions, PBPK models include anatomical and physiological relevant mechanisms, such as the distribution of drugs via blood flow, specific binding, internalization, and release of drug from the cells, excretion, and physical decay.[3,14,18,19] Therefore, by using PBPK models, the determination of the interindividual variability of TIACs and AD can be explained by parameters of the subject (anatomical and/or physiological) and/or the drug. A strategy to individualize treatment is therefore to investigate the source of the interindividual TIACs variability in terms of subject and drug parameters using a PBPK model.

Such strategy can be implemented for example using a SA with a local or a global approach. In the local SA approach, the parameter of interest is sampled based on its variability one-at-a-time (OAT) while fixing other parameters to a certain value. OAT sampling in the local SA method is fast and simple to implement but can lead to misleading results if significant interactions between parameters exist.[20–22] In contrast, a global SA approach perturbs all input parameters of interest in each sampling step and takes into account the interactions between the parameters.[11] In PBPK models, the global SA is more appropriate as it perturbs all parameters within a plausible range and shows the full effect map of the input parameters to the output.[11] The identification of important PBPK model parameters that affect the interindividual variability of TIACs (and thus of ADs) is essential for the individualization of treatment planning in nuclear medicine. Therefore, in this study, we performed a GSA algorithm using the extended Fourier Amplitude Sensitivity Test (eFAST) to identify influential anatomical and/or physiological parameters of a PBPK model that have a large contribution to the interindividual differences of the ADs in ^{177}Lu-labeled prostate-specific membrane antigen (PSMA) targeting therapy to build patient-specific AD treatment schemes. Finally, we show how the information extracted from the GSA can be used to individualize the ADs. This is done by performing simulations that demonstrate how knowledge of the most important parameters identified by the GSA affects the interindividual variability in the kidneys and tumor lesions.

2. MATERIAL AND METHODS

2.A. Biokinetic data, PBPK model, parameters, interindividual variability, and absorbed doses

A population of 13 patients with metastatic castration-resistant prostate cancer who underwent pretherapeutic ^{68}Ga-

PSMA PET/CT (^{68}Ga-PSMA-H-BED-CC) and post-therapeutic planar whole-body scintigraphies after ^{177}Lu-PSMA I&T RLT were used in this study.[23] The Ethics Committee of the Technical University Munich approved the retrospective analysis (permit 115/18 S), and the requirement to obtain informed consent was waived. Anterior and posterior planar whole-body scintigraphies were obtained with a double head gamma camera. The regions of interest (ROIs) were drawn manually over the source organ. The biokinetic data, that is, the time-activity data, were calculated from the organ ROIs using the geometric mean of anterior and posterior counts with the background corrections. The volume of the tumors and kidneys were determined using PET/CT.[19] Two lesions with high uptake and no superimposition with other organs/lesions were selected as tumor one TU1 and tumor two TU2. The remaining tumor lesions were merged into tumor rest TUR.

A previously published[18,19,24] whole-body PBPK model for PSMA-targeting therapy was used as the basic framework for the GSA analysis in this study. In brief, the model includes all physiological and physically relevant mechanisms, such as blood flow, PSMA-specific binding, internalization, and release of ^{177}Lu from the cells, excretion, and physical decay. Labeled and unlabeled peptides are modeled separately. The two models are connected by the competition for binding to the same free receptors and by radionuclide decay. All organs such as kidneys, tumor, salivary glands, liver, spleen, GI tract, prostate, muscle, fat, lung, bone, red marrow, heart, brain, and skin are connected via blood flow. A detailed description of the PBPK model used in this study can be found elsewhere.[18,19,24] The PBPK model for the ^{177}Lu-labeled PSMA-targeting radioligand therapy contains many fixed parameters that have been shown to have a marginal effect to the estimation of individual TIACs.[25] Therefore, the input of interest, as the subject of the GSA analysis, are those parameters which have been estimated from the biokinetic data of the patient population.[18] The list of the investigated parameters in this study is shown in Table I. The log-normal distribution with a Latin hypercube sampling method was chosen for the model parameters, as physiological quantities need to be positive and this distribution was shown to be a good approximation for the investigation of the interindividual variability of the ADs.[26]

The standard MIRD formalism described by Bolch et al.[27] for the calculation of the absorbed dose is implemented:

$$D(r_T) = \sum_{r_s} TIAC(r_s) \times S_{values}(r_T \leftarrow r_s) \quad (1)$$

where $D(r_T)$ is the total absorbed dose in the target organ r_T due to the irradiations from the source organs r_S, $TIAC$ is the time-integrated activity coefficient of the source organ r_S calculated as the ratio of the area under the curve of the time-activity curve and administered activity, and $S(r_T \leftarrow r_s)$ are the S-values of the pair of target r_T and source r_s organ (Supplemental file Table A).[18,28] Self-doses were used for the calculation of the absorbed doses based on S-values of the kidneys and tumors obtained from the OLINDA/EXM software version 1.0.[18,28]

2.B. Global sensitivity analysis

The eFAST was introduced by Saltelli et al.[29] The eFAST test is a variance-based global sensitivity method that is independent of any assumptions regarding model structure (it does not rely on assumptions as to the functional relationship between the model output and its inputs).[29] Although several variance-based global sensitivity methods, such as the Sobol[30] or the top marginal variances (TMV)[31] method, are available, they require a larger number of evaluations than eFAST.[11] A relatively low number of model evaluations and the feature of a good approximation for nonlinear systems

TABLE I. Investigated physiologically based pharmacokinetic (PBPK) model parameters and their corresponding distribution parameters taken from our previous study.[18] The log-normal distribution was used for the simulations to avoid negative PBPK model parameter values.

		Normal distribution		Log-normal distribution	
Parameters	Description	Mean	SD	Mean[a]	SD[b]
$[R_{K,0}]$ (nmol/l)	Receptor density in kidneys	17.61	2.90	2.87	0.16
$[R_{TU1,0}]$ (nmol/l)	Receptor density in tumor 1	44.94	26.87	3.65	0.55
$[R_{TU2,0}]$ (nmol/l)	Receptor density in tumor 2	47.38	29.62	3.69	0.57
$f_{K,C}$ (ml/min g)	Kidney age-independent blood flow	4.26	0.65	1.43	0.15
f_{TU1} (ml/min g)	Flow of tumor 1	0.13	0.11	−2.27	0.74
f_{TU2} (ml/min g)	Flow of tumor 2	0.26	0.45	−1.99	1.16
$\lambda_{Krelease}$ (1/min)	Kidneys release rate	2.26e-4	0.61e-4	−8.43	0.26
$\lambda_{TUrelease}$ (1/min)	Tumor release rate	1.40e-4	5.73e-5	−8.91	0.38
x_f (unitless)	Tumor flow factor	0.53	7.00e-5	−0.63	1.30e-4
x_v (unitless)	Ratio of actual volume to the CT volume	0.64	0.26	−0.52	0.39

[a]Mean of the log-normal distribution calculated as $2 \times ln(mean_{normal}) - 0.5 \times ln(mean^2_{normal} + SD^2_{normal})$.
[b]SD of the log-normal distribution calculated as $\sqrt{ln(mean^2_{normal} + SD^2_{normal}) - 2 \times ln(mean_{normal})}$.

(such as the here used PBPK model) make eFAST the appropriate tool for the GSA analysis. The method provides a way to estimate the expected value E and variance V of the model output and the contribution of input parameters and their interactions to this variance, given physiologically feasible parameter ranges for the inputs. The eFAST technique outputs two types of sensitivity measures, that is, main effects (S_i) and total effects (S_{Ti}). The main effect S_i of an input parameter i represents the reduction in variance of the output if the "true" value of parameter i would be known, for example, the S_i value of input parameter $f_{K,C}$ for the output of ADs to the kidneys shows the relative reduction of the interindividual variability of the ADs in the kidneys if the exact "true" value of $f_{K,C}$ would be known. The total effect S_{Ti} of an input parameter i represents the proportion of variance remaining if the "true" values of all the other parameters $\sim i$ are known: For example S_{Ti} of input parameter $f_{K,C}$ for the output "ADs to the kidneys" shows the interindividual variability of the ADs in the kidneys due to solely the variability of $f_{K,C}$ (because the exact "true" values of all other parameters are assumed known). The calculation of the main effect S_i and the total effect S_{Ti} is a standard practice in GSA.[4,11,29] In this study, the main effect S_i and total effect S_{Ti} of the input parameters of the PBPK model used for treatment planning in PSMA therapy to the interindividual variabilities of the absorbed dose (model output) were quantitatively investigated.

The main concept of the FAST method is the conversion of the k-dimensional integral in Eq. (2) into a one-dimensional integral based on the Weyl theorem.[32]

$$E(Y) = \int_{\Omega^k} f(X)p(X)dX \tag{2}$$

where the expected value of the output $E(Y)$ is calculated by the k-dimensional integral in the input space Ω^k of the product between the model $f(X)$ and the joint probability density function of the input $p(X)$. A unique frequency ω_i is assigned for each input parameter X_i and then transformed according to

$$X_i(s) = G_i(\sin(\omega_i s)), \tag{3}$$

where G_i is the transformation function and s is a scalar variable varying over the range $-\infty<s<\infty$. All the factors are changed along a curve that scans the input space Ω^k for different values of s. Note that the oscillation of X_i only depends on its corresponding ω_i. The model output has its own periodicities combined with different frequencies of the input ω_i and does not depend on the model $f(X)$. Therefore, if the ith input parameter has a strong effect on the model output, the oscillations of the output at the ω_i will have a high amplitude. The k-dimensional integral in Eq. (2) can be estimated by[29]

$$E(Y) = \int_{-\pi}^{\pi} f(s)ds, \tag{4}$$

where $f(s) = f(G_1(\sin(\omega_1 s)), G_2(\sin(\omega_2 s)), \ldots, G_k(\sin(\omega_k s)))$. The total variance of the model output can be approximated by using Fourier analysis:

$$V(Y) = \frac{1}{2\pi}\int_{-\pi}^{\pi} f^2(s)ds - E^2(Y) \approx 2\sum_{j=1}^{N}\left(A_j^2 + B_j^2\right), \tag{5}$$

The function $f(s)$ is symmetric around $s = \pm\pi/2$ for a set of odd frequencies. Therefore, we restricted the range of integration from $(-\pi,\pi)$ to $\left(-\frac{\pi}{2},\frac{\pi}{2}\right)$ halving the number of required evaluations (NE), that is, N_s. In this study, NE is the total number of simulations of the PBPK model using the sampled parameters. The Fourier coefficients were calculated as follows

$$A_j = \frac{1}{N_s}\left\{ f(s_{N_o}) + \sum_{q=1}^{N_q}\left[f\left(s_{N_o+q}\right) + f\left(s_{N_o-q}\right)\right] \times cos\left(j\frac{\pi}{N_s}q\right)\right\}, \tag{6}$$

$$B_j = \frac{1}{N_s}\left\{ \sum_{q=1}^{N_q}\left[f\left(s_{N_o+q}\right) - f\left(s_{N_o-q}\right)\right] \times sin\left(j\frac{\pi}{N_s}q\right)\right\}, \tag{7}$$

where $N_s = (NE+1)/2$, $N_q = (N_s-1)/2$, and $N_o = (N_s-1)/2$. The partial variance of the output due to the effect of input i is approximated by

$$V_i(Y) = 2\sum_{p=1}^{M}\left(A_{p\omega_i}^2 + B_{p\omega_i}^2\right), \tag{8}$$

where M is the number of the maximum harmonic we consider. The main effect S_i of parameter i is calculated as

$$S_i = \frac{V_i(Y)}{V(Y)}, \tag{9}$$

where $V_i(Y)$ is the variance of output Y due to the effect of parameter i [Eq. (8)] and $V(Y)$ is the total variance of output Y [Eq. (5)]. The partial variance of the complementary set of the input parameter is calculated according to

$$V_{ci}(Y) = 2\sum_{p=1}^{M}\left(A_{p\omega_{\sim i}}^2 + B_{p\omega_{\sim i}}^2\right) \tag{10}$$

By using eFAST, the user could estimate the total effect indices (as in the Sobol method) together with estimation of the complementary set V_{ci}. V_{ci} is calculated by assigning a high frequency ω_i for the input of interest i and a low frequency $\omega_{\sim i}$ with maximum values shown in Table II to the

TABLE II. Combinations of the total number of model evaluations and frequencies as suggested in the literature[29] used for the frequency-based sampling in Eq. (3).

Total number of model evaluations (NE)	Frequency of the input of interest i (ω_i)	$\max(\omega_{\sim i})$
129	16	2
257	32	4
513	64	8
1025	128	16
2049	256	32
4097	512	64
8193	1028	128

remaining input. Table II shows all sets of frequencies used in this study. Supplemental File Table B shows the example of sets of frequencies used in this study according to Table II.

The total effect S_{Ti} of input parameter i is calculated as

$$S_{Ti} = 1 - \frac{V_{ci}(Y)}{V(Y)}, \tag{11}$$

where $V_{ci}(Y)$ is the partial variance of the complementary set, calculated using Eq. (10), and $V(Y)$ is the total variance of output Y, calculated using Eq. (5). For the sampling, a frequency-based sampling method for eFAST as suggested by Saltelli et al.[29] was used in this study, that is,

$$X_i(s) = G_i(\sin(\omega_i s)) = \frac{1}{2} + \frac{1}{\pi}\arcsin(\sin(\omega_i s + \varphi_i)), \tag{12}$$

where s is a modified scalar variable varying over the range $-\pi/2<s<\pi/2$, and ω_i is the frequency value used for parameter X_i and φ_i is a random phase-shift chosen uniformly between 0 and 2π. Parameters of interest X_i were sampled from the variability shown in Table II (log-normal). The frequencies show a specific number related to the sinusoidal functions which were assigned to each parameter according to Eq. (12), Table II and Supplemental File Table B. The vector of the input parameters of interest X_i was generated using Eq. (12) with frequency ω_i (Table II). While, the vectors of the complementary parameters $X_{\sim i}$ (all parameters outside the parameter of interest) were generated using Eq. (12) with maximum frequency of $\omega_{\sim i}$ (Table II and Supplemental File B). Note that a new set of model evaluations is needed to compute each of the k complementary variances V_{ci}. Consequently, the total number of PBPK model simulations NE to calculate the main and total effects is

$$k(2M\omega_{max} + 1), \tag{13}$$

where k is the number of the complementary variance, M is the interference factor (factor used to avoid the interference of the frequencies in the sampling)[29] with a value of 4 as suggested in the literature[29] and ω_{max} or (ω_i) is the frequency of input of interest.

2.C. Study workflow

The PBPK model was implemented using Simbiology/MATLAB software version R2019b (MathWorks, Inc., Natick Massachusetts, USA 2019). The outputs of interests for the GSA analysis were the ADs to kidneys and tumor lesions. There were three different types of tumor in the model, that is, two tumors (lesions) TU1 and TU2 and tumor located in the remainder of the body TUR. An in-house program based on the MATLAB software was implemented to calculate S_i and S_{Ti} using the eFAST algorithm[29] as described above. The most important PBPK parameters that strongly affect the interindividual variability of ADs in kidneys and tumors were analyzed for a total injected amount of 100 nmol and an activity of 7.4 GBq. The model input parameters were obtained from previous work (Section 2.A and Table I) and were processed using in-house software for the GSA. The following computational settings were used for the GSA: interference factor M equal to 4 as suggested in the literature,[29] parameters with log-normal distribution to avoid any negative value of the PBPK parameters,[5] Latin-hypercube sampling strategy, and frequency-based sampling method.[29] Figure 1 shows the flowchart of the workflow in this study.

The interindividual variability of the calculated ADs in this study only depend on the variability of TIACs calculated using the PBPK model as the S-values were fixed as suggested in the literature.[4] The main effect S_i and total effect S_{Ti} of parameter i were calculated from the simulated ADs. Model simulations were repeated until the main effect S_i and total effect S_{Ti} of all parameters for certain NE were collected. Increasing numbers of samples NE were calculated, that is, 129, 257, 513, 1025, 2049, 4097, and 8193, to check the stability (i.e., convergence) of the calculated main effects S_i and total effects S_{Ti}.[29] The NE which generated the main effect S_i and total effect S_{Ti} with a difference of less than 1% to the lower consecutive number of the investigated NE was defined as the NE with a converged S_i and S_{Ti}. Finally, simulations were performed to investigate how knowledge of the "true" value of the input parameters with the highest S_i, for example, $f_{K,C}$, $[R_{TU1,0}]$ and $[R_{TU2,0}]$, affects the variability of the ADs in the kidneys and tumor lesions.

3. RESULTS

Figure 2 shows an example of the frequency-based sampling of the population PBPK parameters. The same sampling method was used to investigate the effect of each of the chosen input parameters in Table I on the interindividual variability of the ADs in the kidneys, TU1, TU2 and TUR.

The interindividual variabilities of the ADs in the kidneys, TU1, TU2, and TUR are shown in Fig. 3. The coefficients of variation CV (ratio of the standard deviation to the mean) of the ADs were higher for the tumors compared to the kidneys, that is, (4.9 ± 1.5) Gy, CV = 31%, (15.0 ± 8.3) Gy, CV = 55%, (15.5 ± 9.1) Gy, CV = 59%, and (18.6 ± 7.7) Gy, CV = 41% for the ADs to kidneys, TU1, TU2, and TUR, respectively. The ADs to the kidneys and to the tumor lesions showed a relatively low correlations (correlation coefficient less than 0.1).

Figures 4 and 5 show the effect of the number of model evaluations NE on the estimated S_i and S_{Ti} values, respectively. In most of the cases, NE of about 8193 is needed to assure the convergence of the estimation of the main effect S_i and the total effect S_{Ti}.

The most important PBPK parameters that determine the interindividual variability of ADs in tumor and kidneys were successfully identified using the eFAST method (Fig. 6). For example, the most important three parameters that affect the interindividual variability of the ADs in the kidneys (other parameters had S_i and S_{Ti} less than 10%) were the age-independent kidney flow $f_{K,C}$ (S_i = 0.36, S_{Ti} = 0.43), the receptor density in the kidneys $[R_{K,0}]$ (S_i = 0.25, S_{Ti}=0.30), and the kidneys release rate $\lambda_{Krelease}$ (S_i = 0.23, S_{Ti} = 0.27).

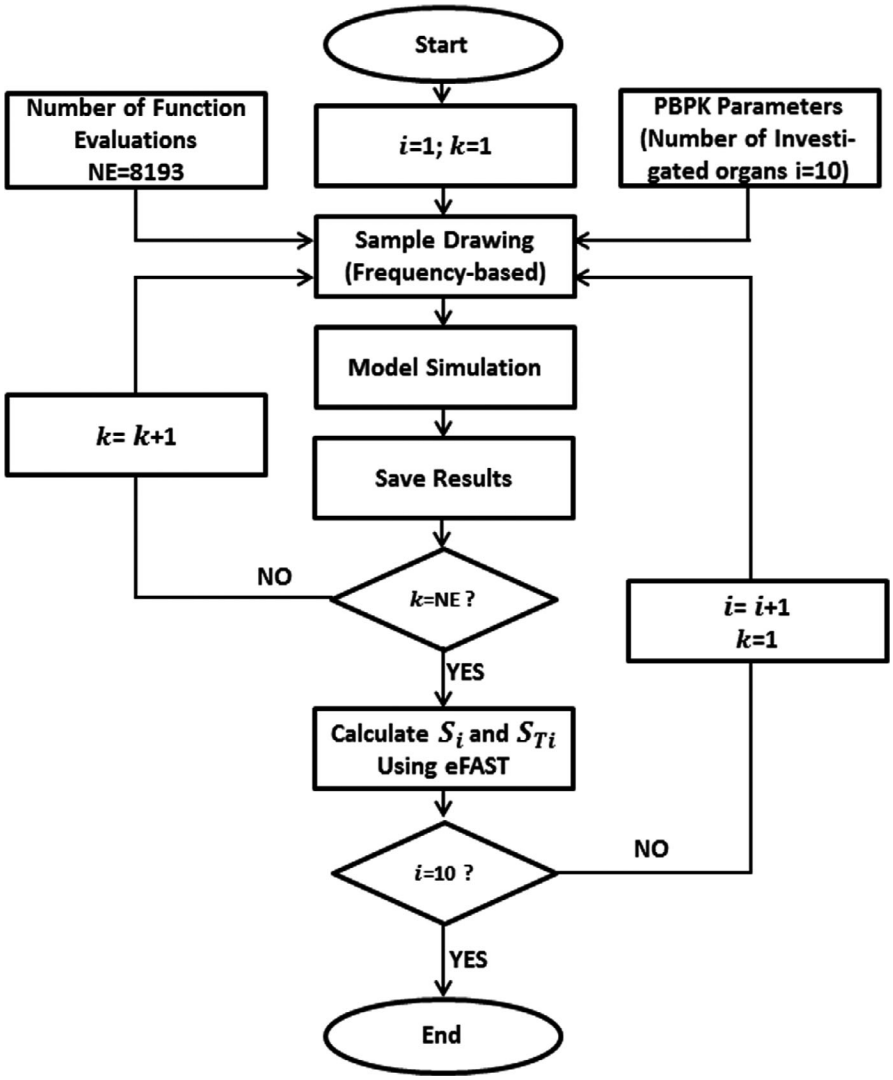

FIG. 1. The flowchart of the workflow in this study. The calculations of the main effect S_i and total effect S_{Ti} were repeated for different NE numbers as shown in Table II. The indices i and k are showing to the input of interest and model evaluations number, respectively. In brief, the parameters (Table I) were sampled using the frequency-based sampling [Eq. (12)] to generate the vectors of input of interest X_i and the complementary set $X_{\sim i}$ for certain number of NE. Total of NE model simulations were performed using the vectors of X_i and $X_{\sim i}$ and the ADs to the kidneys and tumors were calculated from each simulation.

Tumor receptor densities and release rates were identified as the important parameters that determine the interindividual variability of ADs in TU1, TU2, and TUR (other parameters had S_i and S_{Ti} less than 0.1, except for TUR). For example, in TU1: $[R_{TU1,0}]$ ($S_i = 0.59$, $S_{Ti} = 0.71$) and $\lambda_{TUrelease}$ ($S_i = 0.11$, S_{Ti}=0.16), in TU2: $[R_{TU2,0}]$ ($S_i = 0.57$, $S_{Ti} = 0.72$) and $\lambda_{TUrelease}$ ($S_i = 0.11$, $S_{Ti} = 0.17$), in TUR: $[R_{TU1,0}]$ ($S_i = 0.13$, $S_{Ti} = 0.19$), $[R_{TU2,0}]$ ($S_i = 0.17$, $S_{Ti} = 0.24$) and $\lambda_{TUrelease}$ ($S_i = 0.21$, $S_{Ti} = 0.26$).

Knowing the "true" value of $f_{K,C}$ by fixing the number to a certain value, for example, the mean value (Table I), decreased the CV of the variability of the ADs in the kidneys from 31% to 23% (Supplemental File Table C and Fig. 7). This level of decrease in the variability from 31% to 23%, that is, %Diff = 26%, is similar to the predicted level of relative decrease shown by the S_i values, that is, 36%. In contrast, the less important parameters determining the interindividual variability of the ADs in the kidneys predicted by the S_i value, for example, tumor receptor densities were found to have a marginal effect on the %Diff of the ADs in the kidneys (Supplemental File Table C and Figure A). The same results were also found for the ADs to tumors where the percentages of the S_i values were able to reflect the decrease level of the ADs variability %Diff (Supplemental File Table C and Fig. 7). Additional simulations were performed to investigate the effect of fixing the $f_{K,C}$ and $[R_{TU1,0}]$ to the 25th and 75th percentile values to the variability of the ADs in the kidneys and TU1. Again, the relative decreases of the S_i values for the parameters $f_{K,C}$ and $[R_{TU1,0}]$ were also reflecting the decrease level of the variability of the ADs (Supplemental File Table C).

4. DISCUSSION

Individualized therapy planning in nuclear medicine has the potential to improve the treatment outcome.[2,3,5] However,

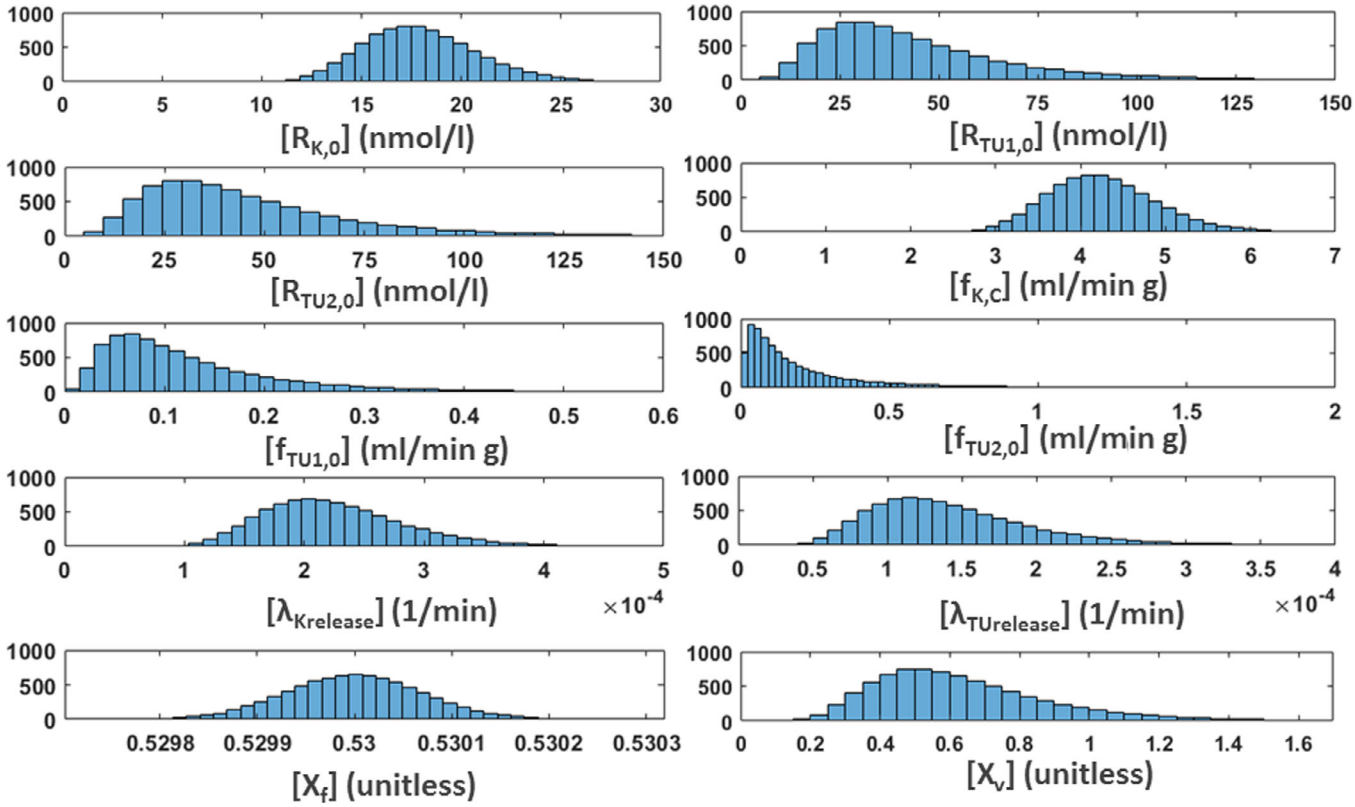

FIG. 2. The histogram of the frequency-based sampling [Eq. (3)] of the PBPK model parameters (Table I) used as the input for the GSA with 8193 evaluations. The sampling was done using the Latin-hypercube sampling strategy and log-normal distribution to avoid negative values. The distributions of the sampled parameters are asymmetrical due to the used log-normal distribution. [Color figure can be viewed at wileyonlinelibrary.com]

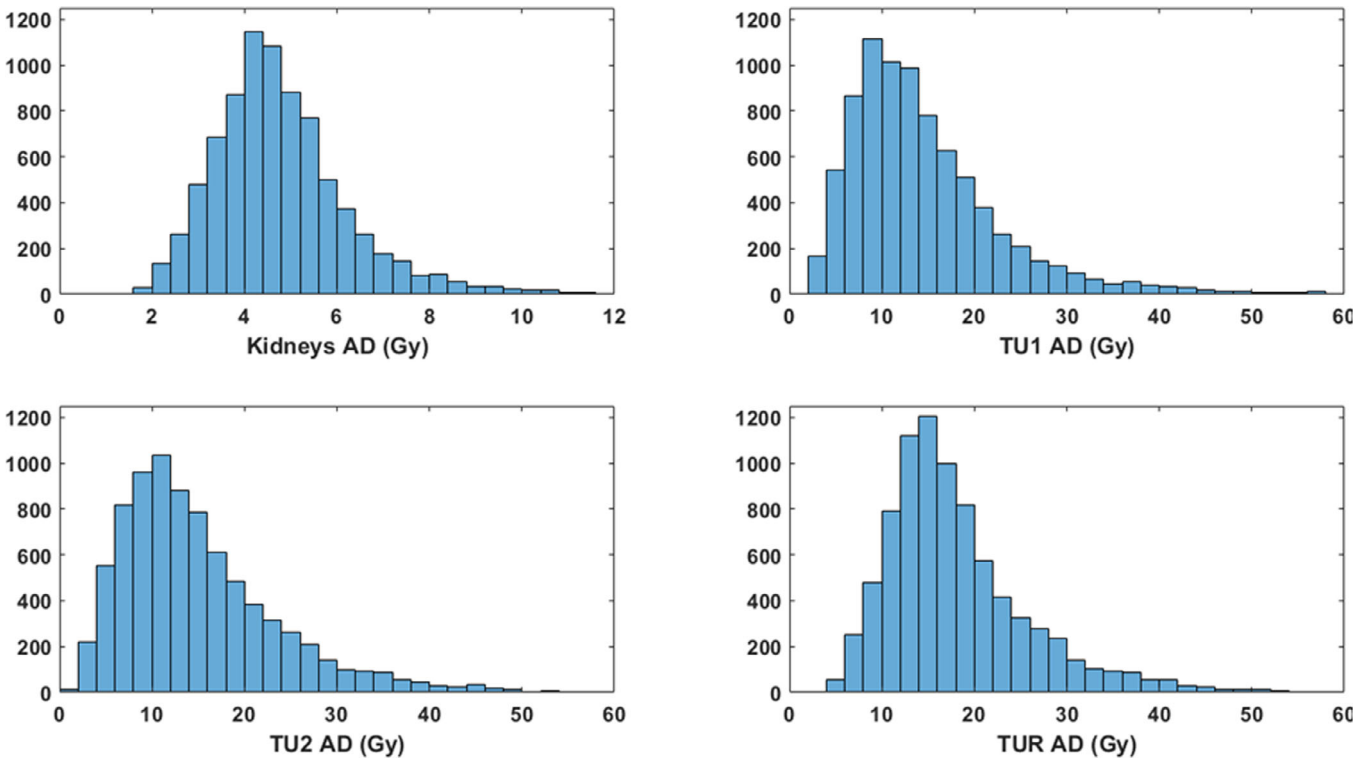

FIG. 3. The histogram of the interindividual variability of the population ADs in the kidneys, TU1, TU2, and TUR generated as the output of the PBPK model using the input parameters. The input of the PBPK model was the sampled parameters (Table I). [Color figure can be viewed at wileyonlinelibrary.com]

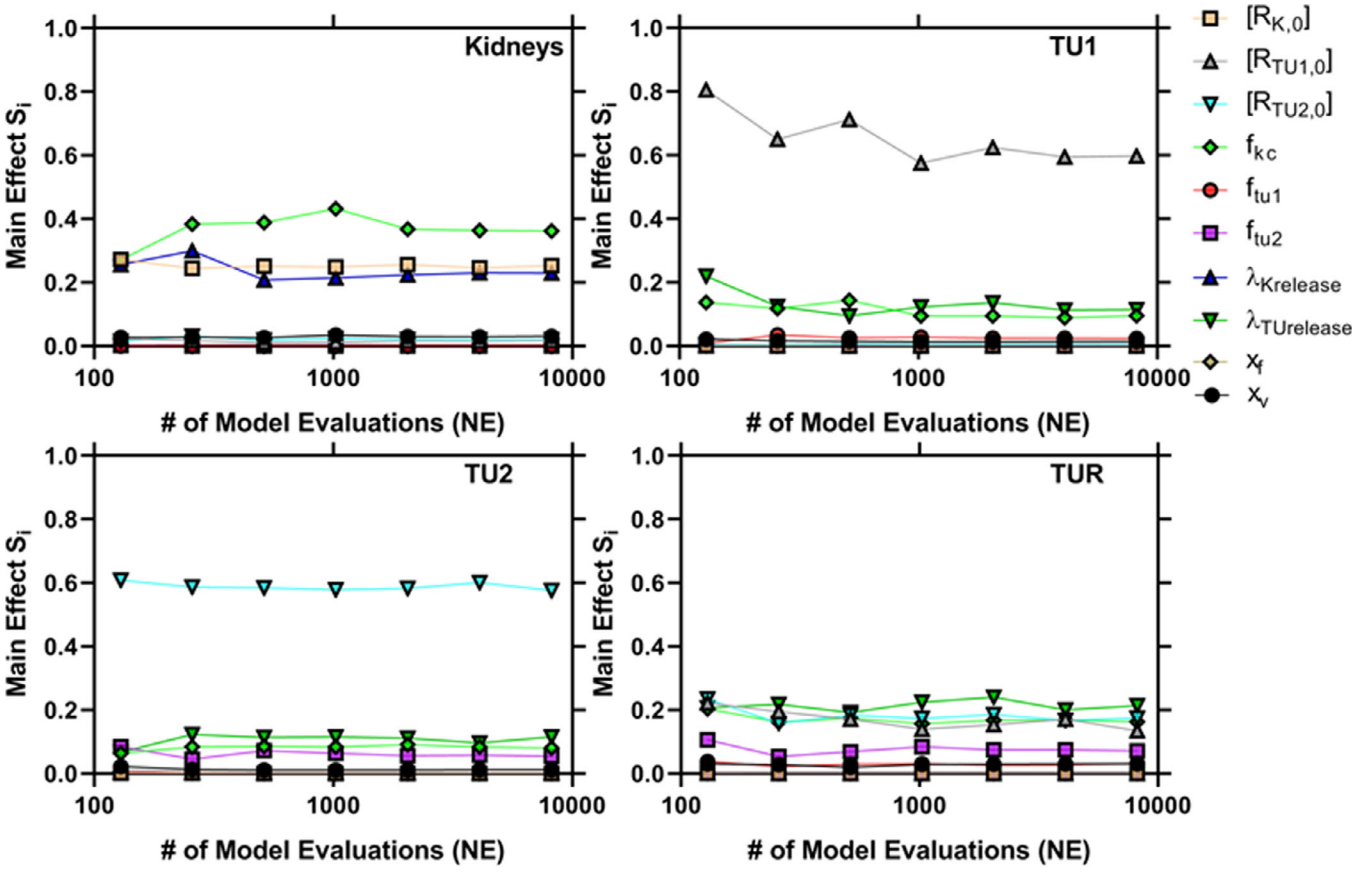

FIG. 4. Convergence of the calculated main effect S_i for kidneys TU1, TU2, and TUR. Various numbers of model evaluation NE and its corresponding frequencies (Table II) were analyzed to ensure the convergence of the calculated main effects S_i and total effects S_{Ti}. [Color figure can be viewed at wileyonlinelibrary.com]

individualized treatment planning is not always feasible in clinical practice due to its complexity and high effort. Therefore, the treatment is often based on a standard activity which will result in a broad distribution of doses in the target organs and the organs at risks in the patient population (Fig. 3). Therefore, a study to investigate the basis of the interindividual variability of the ADs is needed to possibly improve therapy by adapting the treatment planning to the individual patient using individual anatomical or physiological parameters.

In this study, we used a PBPK model and a GSA to investigate the source of TIACs/ADs interindividual variability. By using the PBPK model and a GSA, TIACs and ADs interindividual variability can be explained by the interindividual variability of subject and/or drug-dependent parameters. The PBPK model consists of fixed parameters and of estimated parameters. The latter were obtained from the fit of the PBPK model to individual biokinetic data.18 Our previous study showed a marginal effect of changed fixed parameters to the estimation of individual TIACs.[25] Therefore, in this study, we investigated the effect of the interindividual variability of the estimated parameters (Table I) on the variability of the ADs in ^{177}Lu-labeled PSMA-targeting radioligand therapy using a GSA and a PBPK model.

In this study, we show (a) the application of a GSA for a PBPK model previously developed for ^{177}Lu-labeled PSMA-targeting radioligand, (b) the distribution of the absorbed doses (ADs) in kidneys and tumor in the population, defined by the distribution of the input parameters, in ^{177}Lu-labeled PSMA-targeting radioligand therapy as a result of the PBPK model (Fig. 3), (c) correlations between the ADs in the kidneys and tumor lesions with the physiologic parameters of the patient (Figs. 4 and 5), (d) correlations between the ADs (Supplemental File Figure A), and (e) the effect of knowing an important physiologic parameter identified by the GSA on the uncertainty of the ADs in kidneys, TU1 and TU2 (Fig. 7).

Figure 3 shows the histograms of the ADs in the kidneys and tumor lesions. The interindividual variability of ADs in the kidneys (CV = 30%) is lower than that in tumor (CV up to 59%) in all cases. This result compares favorably with the studies showing a large variation of tumor ADs in patients compared to the organ at risk ADs such as kidneys.[5,28,33] Based on these broad distributions of the ADs to kidneys and tumor lesions in the population, a standard treatment is not optimal for all patients. It is therefore necessary to identify the most important physiological parameters that can reduce this large interindividual variability of AD values. For this purpose a GSA is well suited. Another result showed a weak correlation between the ADs in the kidneys and in the tumor (correlation coefficient less than 0.1).

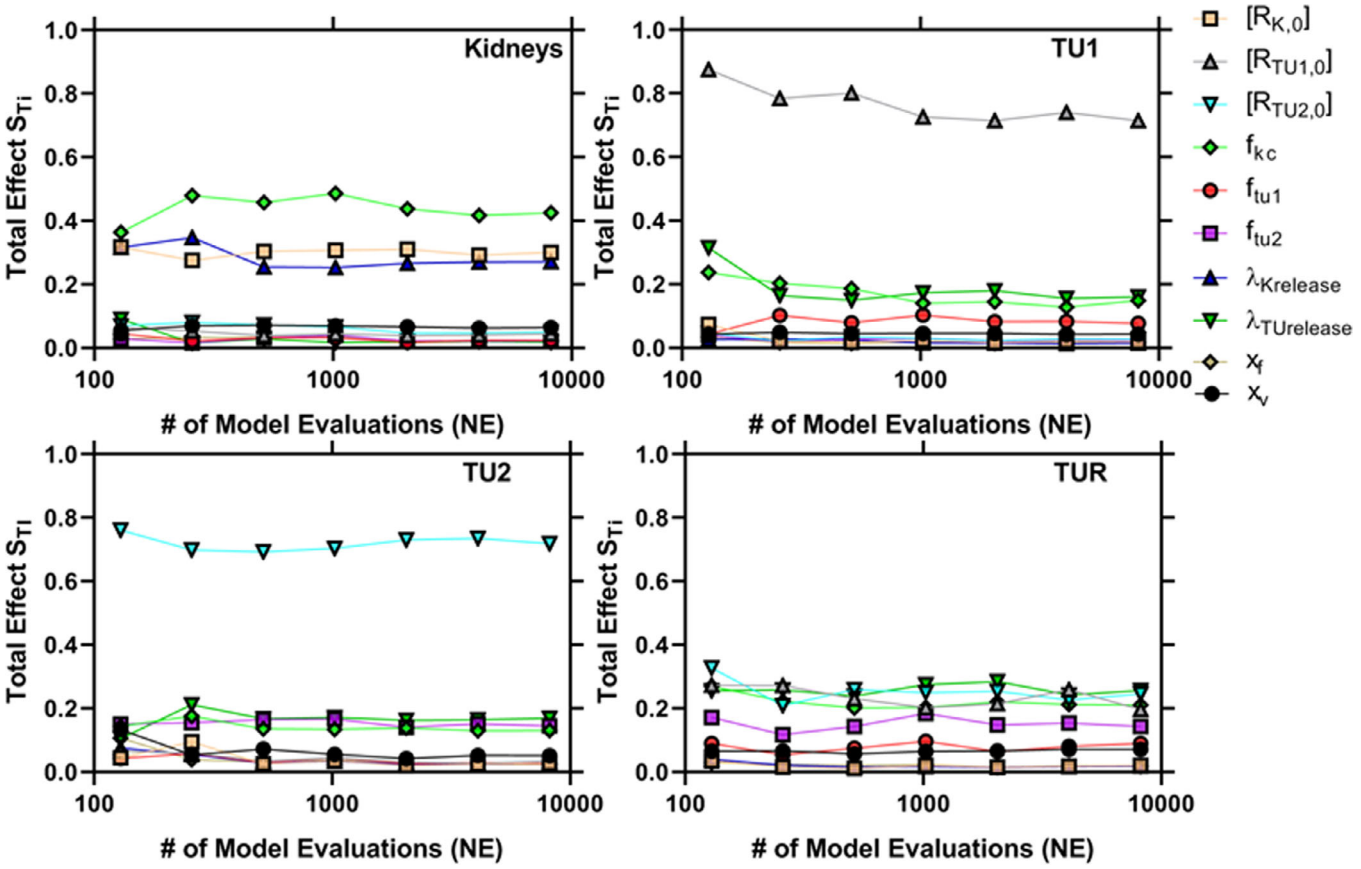

FIG. 5. Convergence of the calculated total effect S_{Ti} for kidneys TU1, TU2, and TUR. Various numbers of model evaluation NE and its corresponding frequencies (Table II) were analyzed to ensure the convergence of the calculated main effects S_i and total effects S_{Ti}. [Color figure can be viewed at wileyonlinelibrary.com]

Based on the convergence test (Figs. 4 and 5), a total number of at least 8193 model evaluation NE is sufficient to converge the calculation of the main effect S_i and total effect S_{Ti} values in all organs. The total number of evaluations needed to converge the S_i and S_{Ti} calculations is considerably higher than that reported by Zvereva et al. (i.e., NE ~ 800).[4] This result is as expected, as a more complex model such as the PBPK model used in this study may increase the necessary total number of evaluations NE[10,29,30] compared to the MIRD model used by Zvereva et al.[4]

A GSA allows attributing the distribution of an output to different inputs. We therefore investigated the most important parameters (inputs) determining the different organ doses (outputs) for a population of thirteen patients treated with a ^{177}Lu-labeled PSMA-targeting radioligand. Based on the used PBPK model together with the elsewhere determined parameter distribution in the population[18] we could identify those parameters which determine the largest differences of absorbed doses in kidneys and tumors between patients and which, therefore, maybe should be taken into account during individualized treatment planning. As a result, we could demonstrate by using the GSA that for an individualized prediction of the kidneys dose the parameter flow $f_{K,C}$ is most important. For the tumor dose the receptor density parameters are most relevant (Fig. 6).

To individualize therapy the inherent variability (i.e., not knowing the individual parameters of a patient) needs to be reduced. In this study, we showed the importance of the organ receptor densities and flows to decrease the variability of the individual ADs during ^{177}Lu-labeled PSMA-targeting radioligand therapy. It has been shown that positron-emission tomography (PET) imaging can be used to measure the cell-surface concentrations of receptors in tumor lesions and kidneys flow.[34,35] Therefore, the organ receptor densities and flows possibly can be determined accurately for an individual patient before treatment with ^{177}Lu-labeled PSMA-targeting radioligands to — partially — individualize the treatment.

Another strategy to reduce the interindividual variability of ADs, instead of directly measuring the flow and receptor density, is to identify further covariates and clinical data (included as Bayesian knowledge or in the nonlinear mixed effect model style) and by measuring the patient prior to therapy. In addition, peri-therapeutic measurements of the first cycle allow to identify important parameters which determine the pharmacokinetics in the later phase and to adapt the remaining cycles accordingly. In Kletting et al.,[19] it has been shown that the receptor density, flow and release rates can be estimated with good accuracy by simultaneously fitting the parameters to PET and therapy data. Some of the parameters can even be determined prior to the first cycle.[3] In

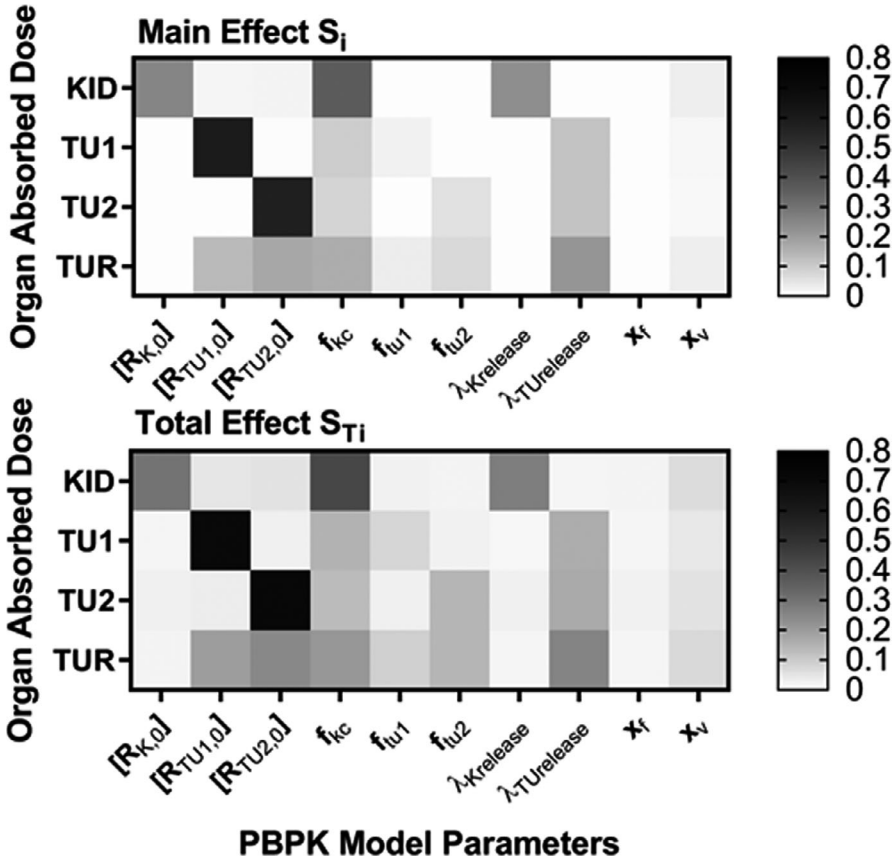

FIG. 6. Map of the main effect S_i and total effect S_{Ti} for all investigated inputs for the variability of the population ADs in kidneys, TU1, TU2, and TUR. In general, parameters related directly to the calculated organ ADs were identified as the parameters with a strong effect to the variability of the population ADs based on the main effect S_i and total effect S_{Ti} values, for example, tumor receptor density $[R_{TU1,0}]$ to the AD in TU1.

conclusion, the GSA can be used to define which parameters need to be measured to individualize therapy, for example, by adapting the injected activity.

A specific PBPK model was used for the analysis.[18,23] Clearly, a fit of a sum of exponentials for each organ or tumor could also have been used. However, in this case a larger number of parameters are needed,[36] which (a) results in a higher uncertainty of each fit parameter and (b) it remains unclear how this specific parameter could be measured (except for the specific fit to the therapeutic time-activity curve which is defining it). This is very different for a PBPK model where the parameters have a physiological meaning and thus could possibly be measured before treatment, for example, by a theranostic PET or SPECT study. Such a measurement is impossible when using the fitting of sums of exponentials due to (a) the short half-lives of the diagnostic radionuclides, (b) the use of different radioligands and (c) different amounts of substances.[8,9] In addition, correlations between the TIACs of different organs and/or tumors are not available. The PBPK model used in this study has been proven to be a relatively "well-suited" model for simulating the biodistribution of a ^{177}Lu-labeled radioligand targeting PSMA based on the physiological parameters.[18,23] Therefore, even if different models exist, the physiological parameters should mostly be the same as they reflect physiological information of the patients.

The main idea of the GSA is to search for important parameters (shown by the main effect S_i and total effect S_{Ti} values) determining the variability of the ADs. Then, for every important parameter one can check, if the possible improvement in therapy justifies the cost of determining these parameters to individualize the treatment planning. In the last part of this study, simulations were performed to show how the variability of the ADs in the kidneys and tumor lesions is reduced when a true value of a parameter is known for a patient. As a result, knowing the true value of the $f_{K,C}$, $[R_{TU1,0}]$ and $[R_{TU2,0}]$ were able to decrease the variability of the ADs in the kidneys and tumor lesions to the level which was predicted by the S_i values. These results show an important benefit of the GSA for the development of individualization in internal dosimetry (at the example of a ^{177}Lu-labeled PSMA-targeting radioligand).

Here, we used the GSA for the analysis of the interindividual variability of the ADs. Curve fitting provides information about the estimated individual ADs. These individual ADs are different between patients. Although the calculation of the interindividual variability of ADs is possible using curve fitting for all patients in a population, identification of the source of the interindividual variability using curve fitting alone is not possible. Here the GSA takes an important part: GSA provides information about the most important

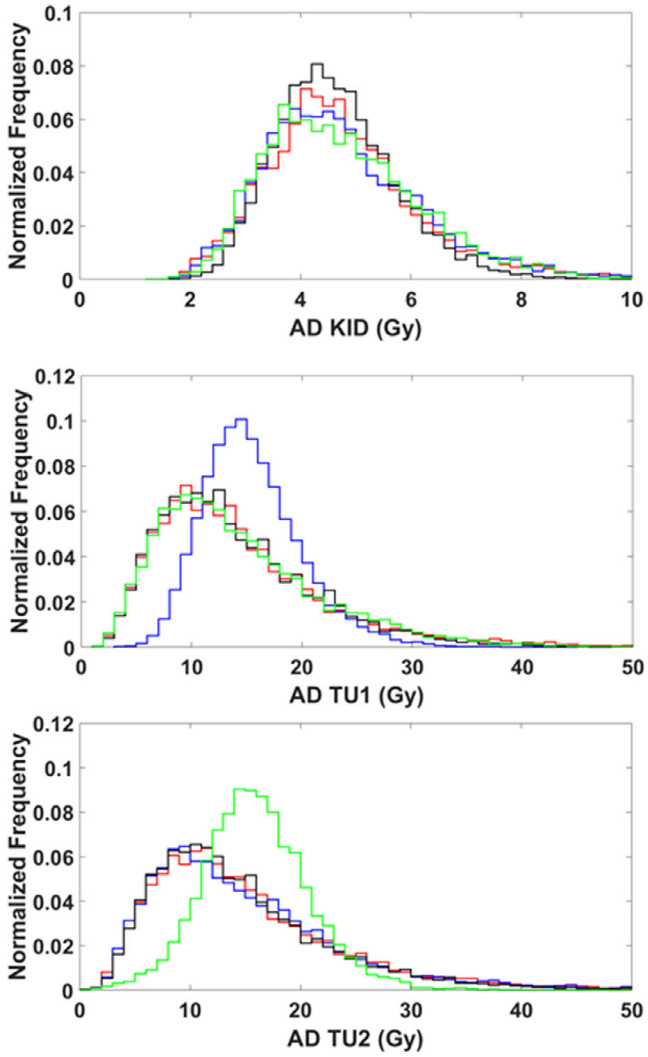

FIG. 7. The normalized histogram showing the effect of knowing the physiologic parameters, that is, $f_{K,C}$ (black), $[R_{TU1,0}]$ (blue), and $[R_{TU2,0}]$ (green), to the interindividual variability of the ADs in kidneys, TU1 and TU2. The original ADs are shown in red. [Color figure can be viewed at wileyonlinelibrary.com]

parameter(s) determining the interindividual variability of the ADs in the kidneys and the tumor lesions in a population which curve fitting can not.

Input, processing and output of the GSA in this study have the following limitations.

For the input of the GSA:

1. A specific PBPK model[18,23] was used for the analysis. Clearly, a model which is more supported by the data could exist. However, as the most important physiological parameters are included in our model, we do not expect that important differences in the results could occur when using such a better PBPK model.
2. The model parameters are assumed to be known in this study, and consequently also the TIACs. Although the intraindividual variability from the uncertainty of an individual dosimetry has been reported to be about 10-20% in several studies,[5,6,26] this is a common assumption.[4] Nevertheless, the performed GSA should yield reliable hypotheses for a knowledge-based individualization approach and thus optimization of treatments in nuclear medicine.
3. The used S-values are not patient specific. Assuming additional distributions for the S-values and including these as input in the GSA would result in a large increase in calculation times. This investigation was not performed as it has been shown that the S-values have a marginal effect to the interindividual variability of the ADs.[4]
4. The model contains fixed parameters, which were assumed to be "true" for all patients. Clearly, this is not the case, however, we have shown earlier a marginal effect of changed fixed parameters to the TIACs due to the fitting of the individual parameters.[25]
5. The population used for the definition of the parameter distribution is relatively small (n = 13). Therefore a study based on a larger population is desired. Nevertheless, the important input variabilities can be calculated, which largely determine the output variabilities.
6. The parameter distributions were assumed to follow a log-normal distribution. Different parameter distributions restricted to positive values could be used, to investigate an effect on the results. We used the log-normal distribution and Latin hypercube sampling that has been shown to be a good approximation for analyzing the interindividual variability of the ADs.[26]

For the processing of the GSA:

1. Other GSA algorithms could have been used. However, a relatively low number of model simulations and the feature of a good approximation for nonlinear systems (such as the here used PBPK model) make eFAST the appropriate tool for the GSA.[11,29]
2. A higher sampling number NE could have been used. However, our investigation of the dependence of the GSA results on NE demonstrated a small change in main and total effect for the used maximum NE = 8193 compared to NE = 4097 (<1%).

For the output there is a limitation that not all interactions of the input parameters were used for the analysis, but only main and total effects. The reason for this is that there would be too many "results" (i.e., all possible interactions for all outputs) which makes the analysis difficult. Therefore, the calculation of the main effect S_i and the total effect S_{Ti} is standard practice in variability studies.[4,11,20,29]

5. CONCLUSIONS

We have shown the first implementation of a GSA for a whole-body PBPK model developed for ^{177}Lu-labeled PSMA-targeting radioligand therapy. By using a GSA, we identified the most important parameters that lead to the broad distributions of the ADs to kidneys and to tumors in

the population (CVs ranged from 31% to 59%). We have shown that the information obtained from the GSA makes it possible to identify those physiological parameters whose knowledge leads to the largest reduction in the uncertainty of ADs. These results show that a quantitative pre- and/or peritherapeutic measurement to precisely determine the individual values of the relevant model parameters may be a possible approach to individualized treatment planning. Thus, based on the PBPK model and the knowledge of these relevant individual parameters, the actual therapy could then possibly be improved by optimizing the activity and the ligand amount administered.

ACKNOWLEDGMENT

This study is supported by collaboration research grant from Universitas Indonesia with contract number NKB-1947/UN2.R3.1/HKP.05.00/2019 and Ulm University, Germany as partner for this research and by the Deutsche Forschungsgemeinschaft (German Research Foundation) under the funding codes KL2742/2-1, BE4393/1-1 and GL236/11-1.

FUNDING

Open Access funding enabled and organized by ProjektDEAL. WOA Institution: Universitat Ulm Blended DEAL: ProjektDEAL

CONFLICT OF INTEREST

The authors have no conflict to disclose.

[a]Author to whom correspondence should be addressed. Electronic mail: gerhard.glatting@uni-ulm.de

REFERENCES

1. Lassmann M, Chiesa C, Flux G, Bardies M, Committee ED. EANM Dosimetry Committee guidance document: good practice of clinical dosimetry reporting. *Eur J Nucl Med Mol Imaging*. 2011;38:192–200.
2. Glatting G, Bardiès M, Lassmann M. Treatment planning in molecular radiotherapy. *Z Med Phys*. 2013;23:262–269.
3. Hardiansyah D, Maass C, Attarwala AA, et al. The role of patient-based treatment planning in peptide receptor radionuclide therapy. *Eur J Nucl Med Mol Imaging*. 2016;43:871–880.
4. Zvereva A, Kamp F, Schlattl H, Zankl M, Parodi K. Impact of interpatient variability on organ dose estimates according to MIRD schema: uncertainty and variance-based sensitivity analysis. *Med Phys*. 2018;45:3391–3403.
5. Stabin MG. Uncertainties in internal dose calculations for radiopharmaceuticals. *J Nucl Med*. 2008;49:853–860.
6. Paquet F, Bailey MR, Leggett RW, Harrison JD. Assessment and interpretation of internal doses: uncertainty and variability. *Ann ICRP*. 2016;45:202–214.
7. Hardiansyah D, Guo W, Attarwala AA, Kletting P, Mottaghy FM, Glatting G. Treatment planning in PRRT based on simulated PET data and a PBPK model. Determination of accuracy using a PET noise model. *Nuklearmedizin*. 2017;56:23–30.
8. Jiménez-Franco LD, Kletting P, Beer AJ, Glatting G. Treatment planning algorithm for peptide receptor radionuclide therapy considering multiple tumor lesions and organs at risk. *Med Phys*. 2018;45:3516–3523.
9. Kletting P, Kull T, Maass C, et al. Optimized peptide amount and activity for 90Y-labeled DOTATATE therapy. *J Nucl Med*. 2016;57:503–508.
10. Saltelli A, Ratto M, Tarantola S, Campolongo F. Sensitivity analysis for chemical models. *Chem Rev*. 2005;105:2811–2828.
11. McNally K, Cotton R, Loizou GD. A Workflow for global sensitivity analysis of PBPK models. *Front Pharmacol*. 2011;2:31.
12. Glatting G, Landmann M, Kull T, et al. Internal radionuclide therapy: the ULMDOS software for treatment planning. *Med Phys*. 2005;32:2399–2405.
13. Strand SE, Zanzonico P, Johnson TK. Pharmacokinetic modeling. *Med Phys*. 1993;20:515–527.
14. Hardiansyah D, Guo W, Kletting P, Mottaghy FM, Glatting G. Time-integrated activity coefficient estimation for radionuclide therapy using PET and a pharmacokinetic model: a simulation study on the effect of sampling schedule and noise. *Med Phys*. 2016;43:5145.
15. Maass C, Sachs JP, Hardiansyah D, Mottaghy FM, Kletting P, Glatting G. Dependence of treatment planning accuracy in peptide receptor radionuclide therapy on the sampling schedule. *EJNMMI Res*. 2016;6:30.
16. Kletting P, Kiryakos H, Reske SN, Glatting G. Analysing saturable antibody binding based on serum data and pharmacokinetic modelling. *Phys Med Biol*. 2011;56:73–86.
17. Kletting P, Kull T, Bunjes D, et al. Radioimmunotherapy with anti-CD66 antibody: improving the biodistribution using a physiologically based pharmacokinetic model. *J Nucl Med*. 2010;51:484–491.
18. Begum NJ, Thieme A, Eberhardt N, et al. The effect of total tumor volume on the biologically effective dose to tumor and kidneys for 177Lu-labeled PSMA peptides. *J Nucl Med*. 2018;59:929–933.
19. Kletting P, Thieme A, Eberhardt N, et al. Modeling and predicting tumor response in radioligand therapy. *J Nucl Med*. 2019;60:65–70.
20. Campolongo F, Saltelli A. Sensitivity analysis of an environmental model: an application of different analysis methods. *Rel Eng Sys Safety*. 1997;57:49–69.
21. Campolongo F, Tarantola S, Saltelli A. Tackling quantitatively large dimensionality problems. *Comput Phys Commun*. 1999;11775–85.
22. Saltelli A.Sensitivity Analysis: From Theory to Practice. In: Global Sensitivity Analysis. The Primer. https://doi.org/10.1002/9780470725184.ch62008:237-275
23. Kletting P, Schuchardt C, Kulkarni HR, et al. Investigating the effect of ligand amount and injected therapeutic activity: a simulation study for 177Lu-Labeled PSMA-targeting peptides. *PLoS One*. 2016;11:e0162303.
24. Begum NJ, Glatting G, Wester HJ, Eiber M, Beer AJ, Kletting P. The effect of ligand amount, affinity and internalization on PSMA-targeted imaging and therapy: a simulation study using a PBPK model. *Sci Rep*. 2019;9:20041.
25. Hardiansyah D, Begum NJ, Kletting P, Mottaghy FM, Glatting G. Sensitivity analysis of a physiologically based pharmacokinetic model used for treatment planning in peptide receptor radionuclide therapy. *Cancer Biother Radiopharm*. 2016;31:217–224.
26. Spielmann V, Li WB, Zankl M, Oeh U, Hoeschen C. Uncertainty quantification in internal dose calculations for seven selected radiopharmaceuticals. *J Nucl Med*. 2016;57:122–128.
27. Bolch WE, Eckerman KF, Sgouros G, Thomas SR. MIRD, pamphlet No. 21: a generalized schema for radiopharmaceutical dosimetry–standardization of nomenclature. *J Nucl Med*. 2009;50:477–484.
28. Stabin MG, Sparks RB, Crowe E. OLINDA/EXM: the second-generation personal computer software for internal dose assessment in nuclear medicine. *J Nucl Med*. 2005;46:1023–1027.
29. Saltelli A, Tarantola S, Chan KPS. A quantitative model-independent method for global sensitivity analysis of model output. *Technometrics*. 1999;41:39–56.
30. Sobol IM. Global sensitivity indices for nonlinear mathematical models and their Monte Carlo estimates. *Math Comput Simul*. 2001;55:271–280.
31. Jansen MJW, Rossing WAH, Daamen RA. Monte Carlo estimation of uncertainty contributions from several independent multivariate sources. In: Grasman J, van Straten G, ed. *Predictability and Nonlinear Modelling in Natural Sciences and Economics*. Dordrecht: Springer Netherlands; 1994:334-343. https://doi.org/10.1007/978-94-011-0962-8_28
32. Weyl H. Mean motion. *Am J Math*. 1938;60:889–896.
33. Stabin MG. Update: the case for patient-specific dosimetry in radionuclide therapy. *Cancer Biother Radiopharm*. 2008;23:273–284.

34. Szabo Z, Xia J, Mathews WB, Brown PR. Future direction of renal positron emission tomography. *Semin Nucl Med*. 2006;36:36–50.
35. Tichauer KM, Wang Y, Pogue BW, Liu JTC. Quantitative in vivo cell-surface receptor imaging in oncology: kinetic modeling and paired-agent principles from nuclear medicine and optical imaging. *Phys Med Biol*. 2015;60:R239–R269.
36. Kletting P, Schimmel S, Kestler HA, et al. Molecular radiotherapy: the NUKFIT software for calculating the time-integrated activity coefficient. *Med Phys*. 2013;40:102504.

SUPPORTING INFORMATION

Additional supporting information may be found online in the Supporting Information section at the end of the article.

Data S1. Supplementary material.

Measure and Evaluate MRgRT 3D Distortion

distortioncheck

CLOUD SOFTWARE FOR EVALUATION OF IMAGE DISTORTION

SCAN

UPLOAD IMAGES

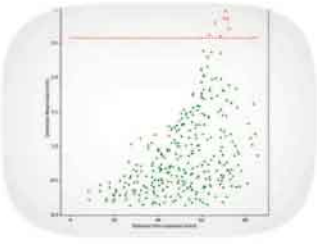

REVIEW REPORTS & TREND ANALYSIS

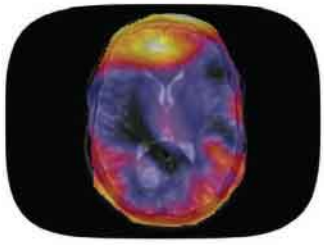

EXPORT DICOM OVERLAYS TO TPS

Large Field Grid Phantom
2152 Physical Control Points

- ✔ CIRS proprietary materials simulate distortion due to susceptibility & chemical shifts typical to clinical patient scans
- ✔ Density of physical control points optimized to bring interpolation close to linearity
- ✔ Cloud based solution frees user of operating system and hardware constraints
- ✔ Quickly & automatically analyze complete MR data sets
- ✔ Online deployment facilitates collaboration, easy review and portability of results

Inter-cranial Grid Phantom
335 Physical Control Points

CIRS
Tissue Simulation & Phantom Technology

cirsinc.com
900 Asbury Ave., Norfolk, VA 23513, USA • (800) 617-1177